ATMOSPHERIC SCIENCE

Secular decrease of wind power potential in India associated with warming in the Indian Ocean

Meng Gao[1]*, Yihui Ding[2], Shaojie Song[1], Xiao Lu[1,3], Xinyu Chen[1]*, Michael B. McElroy[1]*

The Indian government has set an ambitious target for future renewable power generation, including 60 GW of cumulative wind power capacity by 2022. However, the benefits of these substantial investments are vulnerable to the changing climate. On the basis of hourly wind data from an assimilated meteorology reanalysis dataset covering the 1980–2016 period, we show that wind power potential may have declined secularly over this interval, particularly in western India. Surface temperature data confirm that significant warming occurred in the Indian Ocean over the study period, leading to modulation of high pressure over the ocean. A multivariable linear regression model incorporating the pressure gradient between the Indian Ocean and the Indian subcontinent can account for the interannual variability of wind power. A series of numerical sensitivity experiments confirm that warming in the Indian Ocean contributes to subsidence and dampening of upward motion over the Indian continent, resulting potentially in weakening of the monsoonal circulation and wind speeds over India.

INTRODUCTION

India, the third largest energy-consuming country in the world, emitted 2.4 billion metric tons of carbon dioxide (CO_2) in 2013, trailing only China and the United States. The energy supply in India is dominated currently by fossil fuels (73.8%), composed of coal (44.5%), oil (24.2%), and natural gas (5.1%) (*1*). Energy demand in India is projected to increase significantly over the coming decades. Primary energy consumption is forecast to quadruple by 2040 compared to the level that applied in 2005 (*2*). The primary driver is a growing economy expected to reach more than five times its current size by 2040, combined with a demographic boom anticipated to make India the world's most populous country by 2025 (*2*). To match the growing energy demand, approximately 800 GW of new power generation capacity will be required by 2040, equivalent to the existing installed capacity for the entire European Union (*2*).

Wind power is one of the most important alternative energy sources for India, with the potential to decouple the growth of energy demand and emissions of air pollutants and CO_2. Development of wind power in India is relatively recent; its wind capacity amounted to only 6 GW in 2006. The growth since then has been exponential: The cumulative capacity increased by a factor of five in a decade. The cumulative installed capacity for wind power reached 32.8 GW in 2017, ranked number 4 globally, behind only China, the United States, and Germany (*3*). The wind power investment in India is concentrated in western and southern regions, including the states of Tamil Nadu, Gujarat, Maharashtra, and Rajasthan (*4*). These four states account for approximately 70% of the national total (24.3, 16.8, 14.7, and 13.2%, respectively) (*4*). The Indian government has set an ambitious target to double the capacity for wind power over the next 5 years (60 GW by 2022) (*5*). The overall wind power potential for India is 2.5 times higher than its current energy demand (*1*, *6*). The current development of wind power is still at an early stage. Significant expansion of the current capacity will be needed to decarbonize the country's energy economy over the long term.

While wind power provides an important opportunity to mitigate anthropogenic climate change, the available power generation and the economics of wind power investments are also susceptible to a changing climate (*7*, *8*). Projections from climate models highlight prospective declines in wind power potential by 2100 on the order of 10 to 40% over the Northern Hemisphere middle latitudes (*9*). Sherman *et al.* (*10*) argued that the potential for wind power in China has been declining markedly over the past 37 years; the decline attributed primarily to weakening of the East Asia winter monsoon. The presence of a high-pressure system over Siberia in combination with variations of pressure associated with changes in temperature over the Western Pacific represents the dominant influence for the winter wind regime in China. Conditions determining wind power potential in India differ from those in China. Blocking due to the presence of the Tibetan Plateau in combination with the seasonal distribution of temperature in the Indian Ocean is especially important for India. The potential variation of wind power resources and possible links to a changing climate in India are underappreciated. Insights on this topic are critical, as wind power investments are expected to play an increasingly important role in satisfying India's growing energy demand.

In this study, we report an analysis of variations in wind power potential for India over the past four decades, with a focus on relevant driving climate factors. Following Sherman *et al.* (*10*), a high-resolution assimilated meteorology dataset for wind speeds [Modern-Era Retrospective analysis for Research and Applications, version 2 (MERRA-2)] was adopted to explore the potential wind power output for India, with an hourly time resolution and a spatial resolution of approximately 50 km by 50 km. We find that India has been experiencing a significant reduction in the potential for wind power generation (−0.77 PWh per decade; $P < 0.01$) over the study period, primarily in spring and summer. The dominant influence responsible for the decreasing wind potential is attributed to strong warming in the Indian Ocean, resulting in a weakening of the Indian summer monsoon (ISM). This association is validated further on the basis of a statistical model and with simulations using a regional numerical climate-weather model.

[1]School of Engineering and Applied Sciences, Harvard University, Cambridge, MA 02138, USA. [2]National Climate Center, Chinese Meteorological Administration, Beijing 100081, China. [3]Department of Atmospheric and Oceanic Sciences, School of Physics, Peking University, Beijing 100871, China.
*Corresponding author. Email: mgao2@seas.harvard.edu (M.G.); xchen@seas.harvard.edu (X.C.); mbm@seas.harvard.edu (M.B.M.)

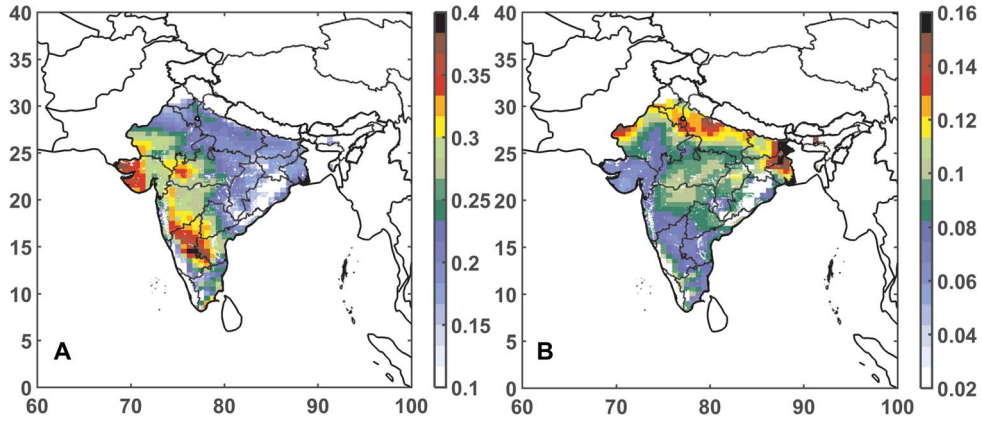

Fig. 1. Spatial features of wind resources. Spatial distribution of (**A**) 37-year mean CFs and (**B**) the CV (defined as the ratio of the SD to the means).

RESULTS

Wind power spatial distribution

Figure 1 (A and B) shows mean values of capacity factors (CFs; more details in Materials and Methods) for wind power and related coefficients of variation (CVs; based on annual values) for India during the 1980–2016 period. High-quality wind resources are located predominantly in western and southern India, with CF values higher than 25%. Compared with the global CF map shown in Lu *et al.* (*6*), values of CF calculated for India in this study are generally higher but with a similar spatial distribution. Lu *et al.* (*6*) used the Goddard Earth Observing System Model, version 5 (GEOS-5) six-hourly operational meteorology dataset, while this study uses the more recently updated MERRA-2 hourly assimilated fields, the likely source of the differences. Further, MERRA-2 covers a longer time period compared to GEOS-5. Northern and central Indian regions are associated with a high interannual variability, with values for CVs higher than 10%. The implications of these interannual variations are detailed later in the Discussion section.

Long-term wind power variability

We calculated a 37-year mean potential electricity (PE) generation for five regions: western, northern, southern, eastern, and northeastern India, as presented in Fig. 2A. The spatial distribution of wind power in India is extensive: Western India accounts for the largest share (36%) of the national total, followed by northern and southern India (26 and 25%, respectively). Northern and western India are found to show the greatest declines (−18 and −14.4%) over the past several decades, with reductions of −5.0 and −4.0% per decade, respectively. In the states with the largest installed wind power capacity, significant declines are found as well, with the exception of the results for Tamil Nadu. The greatest decline is projected for Rajasthan, where PE generation is highest (Fig. 2B). The long-term declining trend of the wind resource poses a potential risk for the financial return on wind power investments. The current investment accounts only for 2 to 3 years of historical wind conditions, but the lifetimes of a wind turbine range from 20 to 30 years (*11*, *12*). A potential secular decline of wind conditions triggered by climate change, in this case, could influence the future financial return of recent wind investments.

Over the entire Indian subcontinent, PE production decreased at a rate of −0.77 PWh per decade [$P < 0.01$; −13% during the 1980–2016 period (Fig. 3A)], suggesting that wind power systems installed over this time interval would have become less productive.

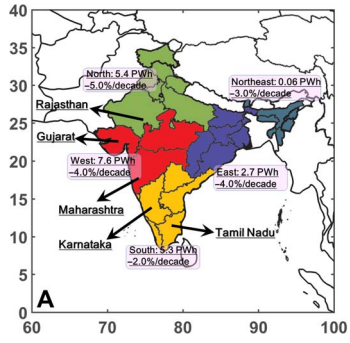

States	Trend (PWh/decade)	37-year mean (PWh)
Tamil Nadu	0.00	1.05
Maharashtra	−0.11	2.84
Gujarat	−0.04	2.02
Rajasthan	−0.17	3.12
Karnataka	−0.03	1.88

B

Fig. 2. Spatial features of declines in PE generation. The 37-year mean potential for electricity generation from the wind and declining rates inferred for western, northern, southern, eastern, and northeastern India (**A**) and a summary of results (**B**) for selected states with large wind power investments.

In India, 63% of the annual production of electricity from wind is contributed by winds in spring and summer (Fig. 3B). However, the PE that could be generated from winds in spring and summer has been declining rapidly, with rates of decline higher than those in fall and winter. The secular decrease in wind power in India, particularly during spring and summer, reflects weakening of the ISM over the study interval.

Warming in the Indian Ocean and declining temperature contrast

The contrast between low pressure associated with high temperature over the Indian subcontinent and high pressure over the ocean drives the ISM (*13*). The Mascarene High in the southern Indian Ocean (SIO) is the powerhouse of the ISM. Winds originating from this system turn to the northeast under the cross-equatorial pressure gradient force. The flow from the Southern Hemisphere can also form closed or almost closed circulation patterns near the equator, systems referred to as equatorial anticyclone/highs (*14*). The sinking air in the lower troposphere near the equator confirms the existence of equatorial anticyclone/high (fig. S1). We calculated trends in surface temperature during the monsoon season [May, June, July, and August (MJJA)] in the Indian subcontinent, the equatorial Indian Ocean (EIO), and the SIO (regions are marked in Fig. 4A) using the surface temperatures developed in MERRA-2. Figure 4B shows the time series of temperature averaged over these three regions during the study interval. Mann-Kendall trend analysis was applied to examine the significance of the temperature

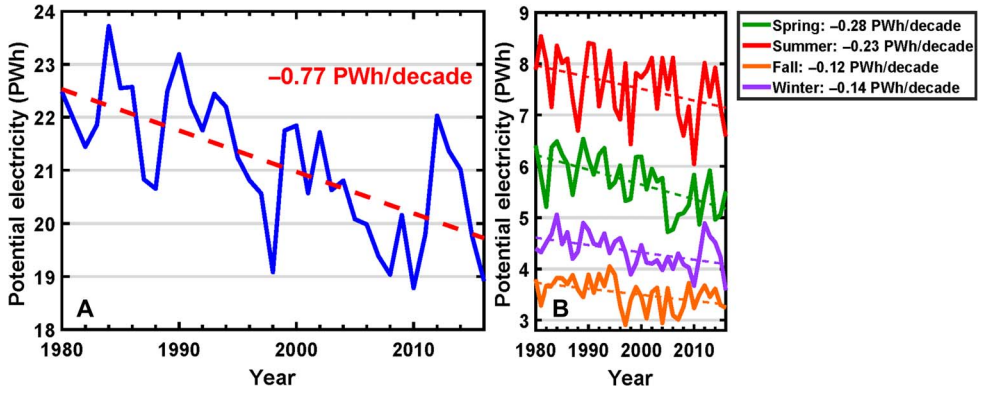

Fig. 3. Interannual and seasonal features of declines in PE generation. Time series for (**A**) the total PE generation over the 1980–2016 period and (**B**) the seasonal PE generation, including a linear fit.

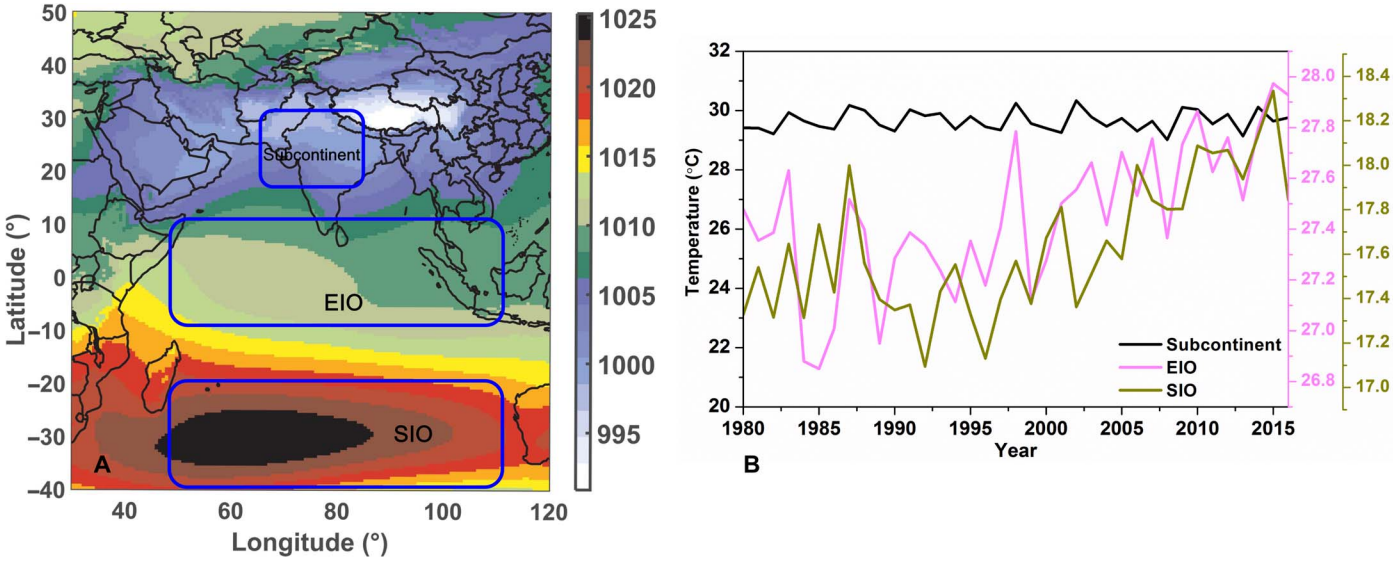

Fig. 4. Decadal trend of temperature for specific regions. MERRA-2–derived spatial distributions of (**A**) SLP for MJJA averaged over the 1980–2016 period and (**B**) time series of temperature averaged over the Indian subcontinent, EIO, and SIO (regions marked with blue boxes on the left).

trend with a P value of less than 0.05. There was no significant trend for temperature over the Indian subcontinent (65°E to 85°E and 15°N to 30°N), while temperature over the EIO (50°E to 110°E and −10°S to 10°N) and the SIO (50°E to 110°E and 20°S to 40°S) regions increased significantly ($P < 0.01$). Warming in the Indian Ocean implies that the land-sea thermal gradient was declining over the study period, serving to modulate the strength of the ISM. A recent study using a coupled model framework points out that warming over the equatorial ocean inhibits convection over the Indian subcontinent, suppressing rainfall over India and modulating the Hadley circulation (*15*).

Figure 5 (A and B) shows temperature and sea-level pressure (SLP) differences between the EIO and the Indian subcontinent (A) and between the SIO and the Indian subcontinent (B). As the temperature contrast between the EIO and Indian subcontinent decreases ($P < 0.01$), the SLP gradient declines significantly ($P < 0.01$). However, although similar trends are found for the temperature contrast and for the SLP gradient between the SIO and the Indian subcontinent, the SLP gradient trend fails to pass the significance test ($P = 0.46$).

We developed a multivariable regression statistical model incorporating dP_{slp1} (SLP differences between the EIO and Indian subcontinent) and dP_{slp2}(SLP differences between the SIO and the Indian subcontinent) and time t to represent potential wind electricity generation

$$PE = a_0 + a_1 dP_{slp1} + a_2 dP_{slp2} + a_3 t$$

where a_0, a_1, a_{20}, and a_3 denote regression coefficients obtained through optimization. This statistical model was applied to the entire Indian region for spring and summer when the ISM is prevalent. Figure 5C shows the annual PE predicted for the spring and summer seasons on the basis of the multivariable statistical model with wind speeds derived from MERRA-2. The statistical model accurately reproduces the descending trends in spring and summer electricity generation, with a correlation coefficient as high as 0.84 ($P < 0.01$). This suggests that the gradient of pressure between sea and land during the monsoon season can effectively determine the wind electricity generation potential in spring and summer. Since the wind potential for India is dominated by conditions in spring and summer (Fig. 3B), and the spring and summer wind potential is highly correlated with annual wind potential ($r = 0.94$, $P < 0.01$; Fig. 5D), the regression model based on the pressure

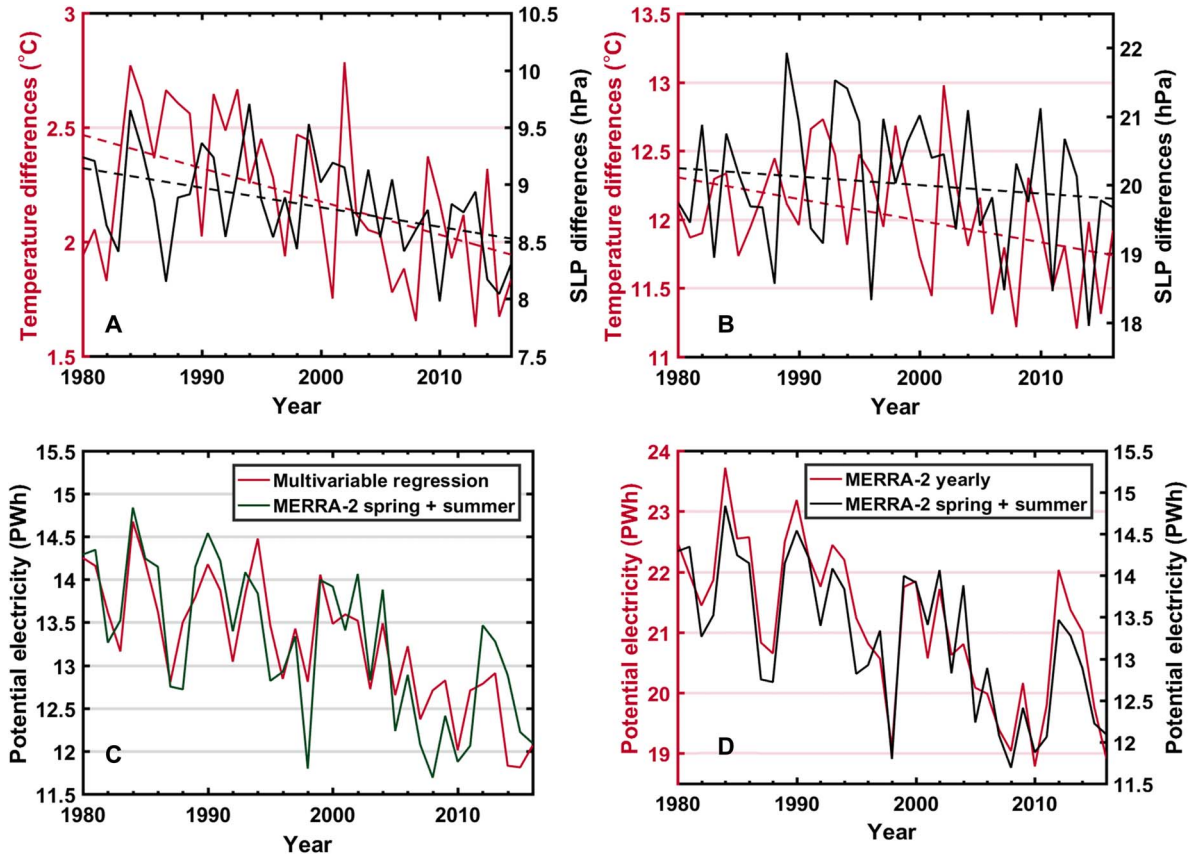

Fig. 5. Temperature and SLP contracts between land and ocean. Temperature and SLP differences between the EIO and the subcontinent (**A**) and between the SIO and subcontinent (**B**), with results from the linear regression model (**C**) and the correlation between yearly PE and spring and summer PE (**D**).

gradient in the monsoon season (MJJA) displays considerable skill in reproducing and predicting long-term interannual trends for wind power potential in India.

Numerical model response to warming in the Indian Ocean

To examine the role of warming in the Indian Ocean on wind speeds at wind turbine hub height, we conducted numerical model sensitivity experiments using the Weather Research and Forecasting (WRF) model. Figure 6 (A and B) shows the response of model wind speeds at 100 m to warming over the EIO regions (A) and to warming over both the EIO and SIO regions (B). Warming over the EIO results in a decline in wind speed at 100 m over northern and southern India, but with no apparent change in western India (Fig. 6A). As shown in Fig. 2A, western India experienced a significant decrease in potential wind power. When warming over both the EIO and SIO regions is taken into account, the reduction of wind speed at 100 m over India is further enhanced, particularly over western India. The response of model wind speeds at 100 m to warming over both regions shows better spatial agreement with the trend of lower troposphere wind speeds in MERRA-2. Declines in wind speeds at 15°S inferred from MERRA-2 (fig. S2) are consistent with the model responses to warming over both EIO and SIO regions but are not seen in the model responses to warming only over the EIO region (Fig. 6, A and B). This further confirms the conclusion that the interannual variability of wind power potential over India is affected jointly by warming over both the EIO and SIO regions.

Examination of changes in vertical wind velocity over the Indian subcontinent and the Indian Ocean region (50°E to 80°E) due to warming in the Indian Ocean is shown in Fig. 6 (C and D). Significant warming over the EIO is responsible for large-scale upward motion over this region, extending up to and spreading over the upper troposphere (Fig. 6, C and D). This large-scale motion favors subsidence in the Southern Hemisphere (20°S to 40°S; Fig. 6C) but is compensated by warming over the SIO, as indicated by the less intensified downward motion at 30°S (Fig. 6D). The warming over the EIO leads also to subsidence of air over the Indian subcontinent (15°N to 30°N), inhibiting convection over land and, thus, reducing the intensity of the monsoonal circulation.

DISCUSSION

Analysis of the spatial and long-term variability of wind power potential in India using assimilated meteorology indicates that there would have been a significant decline over the past 37 years, particularly in the highly invested western Indian region (Rajasthan and Maharashtra states). Nationwide planning for future wind power investments in India could be usefully informed by consideration of the historical reconstruction.

The variation of wind power potential for India is attributed mainly to changing properties of the ISM, modulated by trends in sea surface temperature (SST) in the Indian Ocean. SST in the Indian Ocean increased significantly during the study period (1980–2016). Both statistical and numerical model analyses confirm that warming in the

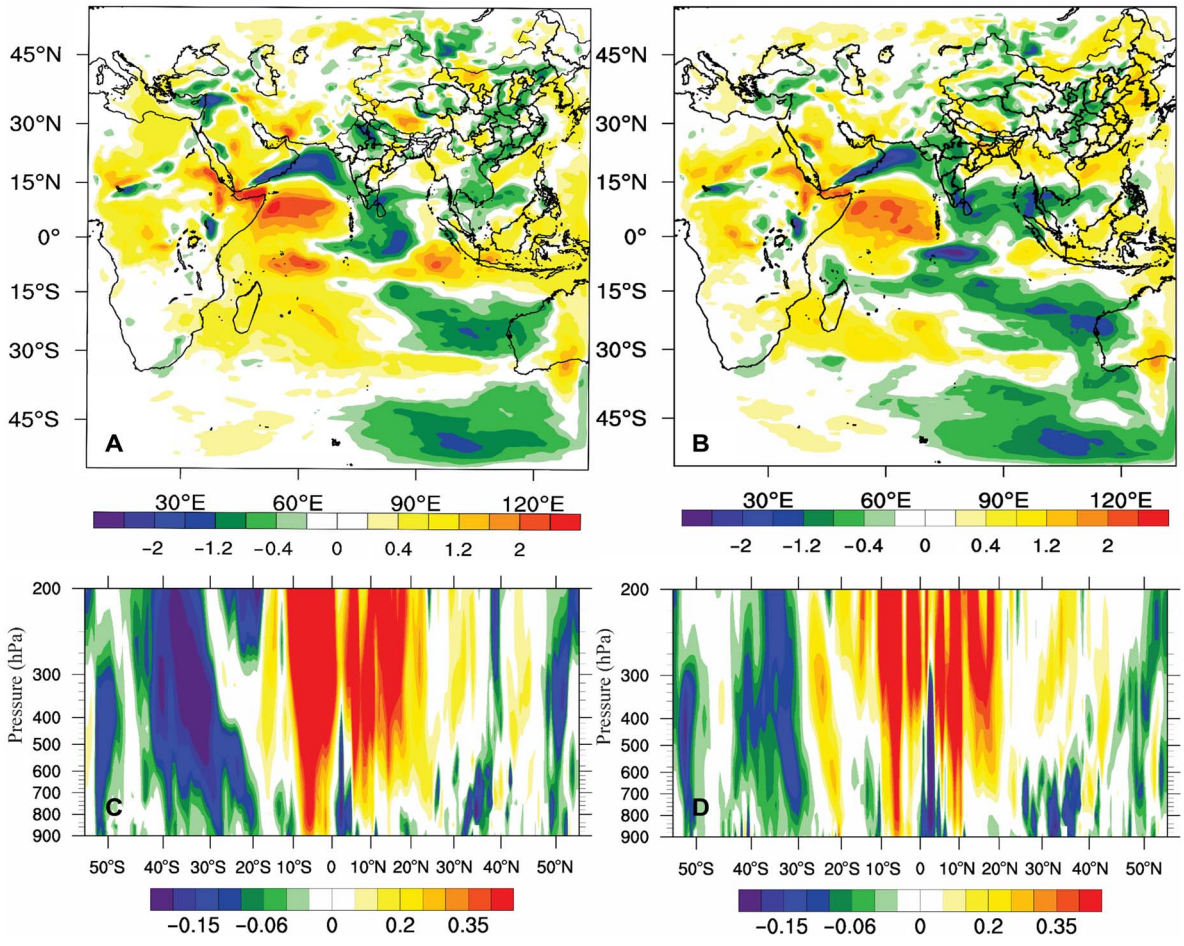

Fig. 6. Model responses to warming in the Indian Ocean. Climate model response of wind speeds at 100 m (**A** and **B**) and zonal mean (60°E to 80°E) cross section for vertical wind speeds (**C** and **D**) to warming over the EIO (left column) and over both the EIO and SIO (right column).

Indian Ocean contributed to a weakening of the intensity of the ISM, resulting in a decline of wind power potential for India as a whole.

The Indian Ocean and the ISM are closely linked: Enhanced warming in the Indian Ocean has been implicated in a reduction of ISM rainfall (*15*, *16*); conversely, weakening of the summer monsoonal cross-equatorial flow has contributed to an acceleration in Indian Ocean warming (*17*). Many studies have been conducted to elucidate mechanisms for this Indian Ocean warming. Positive Indian Ocean warming is found to be associated largely with anthropogenic forcing, enhanced by greenhouse gases (GHGs), but weakened by anthropogenic aerosols (*18*–*20*). Rao *et al.* (*20*) found that the net surface heating resulting from GHGs is not sufficient to account for the consistent warming, while intensified convection over the EIO has exerted a consistent positive feedback on warming over the ocean. Lee *et al.* (*21*) argued that the recent warming trend in the Indian Ocean has its origin in the Pacific Ocean, the influence communicated by the Indonesian throughflow.

Although our analysis indicates that the weakening of the ISM has been implicated as having a negative impact on the historical variation of power from wind, there has been an intense debate on the stability of the ISM. Goswami *et al.* (*22*) showed that extreme ISM rain events increased significantly between 1951 and 2000, while moderate events decreased. Jin and Wang (*23*) reported that, since 2002, ISM rainfall showed a revival driven by stronger warming over land and less warming in the Indian Ocean. This monsoonal strength revival is not seen, however, in our wind power analysis. On the basis of simulations of future climate, Ma and Yu (*24*) found that the ISM may be weakening in the upper troposphere but strengthening in the lower troposphere in response to enhanced surface land-sea thermal contrasts. However, the enhanced land-sea temperature contrast under increasing GHGs forcing is not apparent in the analyses of historical temperature trends (*15*, *23*). The mismatch between predictions based on radiative forcing of GHGs and observed historical land-sea temperature contrast has been attributed to an offsetting negative influence from aerosols over the Indian subcontinent (*25*–*27*). The competing effects of GHGs warming and aerosol cooling may have contributed to the minor trend in temperature observed over the Indian subcontinent (Fig. 4B).

This study emphasizes the impact of Indian Ocean warming on wind power. It does not, however, exclude the possibility of other factors, such as surface roughness changes (*28*) and teleconnections from remote regions. Previous studies highlighted the importance of the Atlantic multidecadal oscillation (AMO) on Indian rainfall (*29*–*32*) and suggested that an anomalously warm North Atlantic and cold South Atlantic could contribute to a strong ISM. However, the AMO shifting from the cold to warm phase during this study interval (1980–2016) should have resulted in an enhancement in the ISM, but this work, along with other previous studies, fails to support this conjecture (*15*, *23*).

The variable wind power will affect decisions made at all timescales and across multiple geographic scales associated with the planning and operation of power systems (*33*). Different time frames need to be addressed when examining the impacts of integrating intermittent wind power. On the time frame of seconds to minutes, the system operation is controlled mainly by automatic equipment and control systems (*34*). From a time frame of minutes to 1 week, system operators need to commit and dispatch generators to maintain power balance through normal conditions and to deal with contingencies (*34*, *35*). On annual-to-multiyear time frames, system planners must ensure that transmission and generation facilities can provide reliable power at low costs under emission constraints (*34*). In addition, several important environmental and climate policies, such as carbon reduction targets, renewable portfolio standards, and carbon cap-and-trade initiatives, are mainly designed and evaluated on a yearly timescale.

The impacts of short-term variability of wind power on system operations, including unit commitment, economic dispatch, and operational reserves, are consequential but relatively well understood. We note that the interannual variability discussed in this paper is not directly linked to the short-term power system operation. However, the impacts of interannual variability of wind power on a longer time frame have been underappreciated (*36*) until recently. A recent study (*36*) combined power system long-term planning with 10 years of interannual variation of renewables for the first time. It pointed out that the interannual variability of climate conditions significantly affects the planning and operation of power systems with respect to the levelized cost of electricity and CO_2 emission intensities in the United Kingdom under medium and high penetration of renewables. Another recent study (*37*) pointed out further that the volatility of annual total generation cost and emission intensity for European power systems (due to interannual climate variations) will increase by a factor of 5 when the renewable penetration increases to 35% as compared to the condition that applied in 2015. The design of carbon policies, for instance, should allow for the banking of renewable credits/carbon allowances over more than a year to hedge against this interannual variability.

The relationship between warming of the Indian Ocean and wind power in India could help improve the understanding of interannual variations. Predictions of the power available from wind over the coming year can be improved on the basis of the forecasts of the SST anomaly. For example, the current National Oceanic and Atmospheric Administration forecast for SST anomalies projects that significant changes in SST in the Indian Ocean are not expected to develop in 2018 (*38*), suggesting little change in expected wind power generation for India this year. Karnauskas *et al.* (*9*) concluded that the wind energy resource will increase in India over the next century based on CMIP5 (Coupled Model Intercomparison Project Phase 5) models. Given the fact that most of these models failed to simulate the spatial distribution of aerosols over India (*27*), nor did they capture land-sea temperature contrasts, it is clear that these projections should be interpreted with caution. The present study provides insights on how warming in the Indian Ocean historically affected wind power in India. Focused studies of factors influencing thermal conditions in the Indian Ocean could play an important role in projections for the future potential of wind power.

MATERIALS AND METHODS

CF and PE generation analysis

The power curve for the GE 2.5 MW wind turbine was applied in this study to calculate hourly wind power outputs. The hub height of the GE 2.5 MW wind turbine is 100 m. Previous studies estimated wind speeds at hub height through interpolation using the oversimplified $^1/_7$ coefficient that ignores the variation due to changes in surface roughness or atmospheric stability (*39*). We obtained wind speeds at 10 and 50 m from the NASA MERRA-2 dataset, a replacement for the MERRA dataset with more observational constraints (*40*). MERRA-2 provides hourly wind speeds at 10 and 50 m on a grid of 0.5° latitude by 0.625° longitude. Wind speeds from MERRA-2 were validated using four reanalysis datasets [National Centers for Environmental Prediction (NCEP)/National Center for Atmospheric Research Reanalysis-1, NCEP/Department of Energy Reanalysis-2, ERA-Interim reanalysis, and MERRA reanalysis] and measurements of wind speeds at 10 and 100 m in India (section S1). Validations at both near-surface levels and 100 m displayed consistent declining trends. We used Eqs. 1 and 2 (*10*, *39*, *41*) to estimate the friction coefficient (α) and wind speeds at 100 m (v_{100})

$$\alpha = \frac{\ln \frac{V_{50}}{V_{10}}}{\ln \frac{50}{10}} \quad (1)$$

$$v_{100} = V_{10}\left(\frac{100}{10}\right)^{\alpha} \quad (2)$$

Estimated hourly wind speeds at 100 m were substituted into the power curve for the GE 2.5 MW wind turbine to calculate hourly wind power outputs and hourly CFs. CF values are defined by

$$\mathrm{CF} = \frac{P_{\mathrm{real}}}{P_{\mathrm{rated}}} \quad (3)$$

where P_{real} denotes the real hourly wind power output and P_{rated} refers to the rated power of the turbine. To eliminate areas judged unsuitable for deployment of wind power systems, such as regions that are forested, urban, or covered with water or ice, we used land cover information obtained from the NASA MODIS (Moderate Resolution Imaging Spectroradiometer) satellite MCD12C1 dataset (*42*). The SRTM 90m digital elevation database version 4.1 (*43*) was used to calculate terrain elevation and slopes for each grid. Grids characterized by slopes of more than 20% or by heights of more than 3000 m were excluded as inappropriate for deployment of wind power systems. We assumed that the turbines should be separated by approximately 9 by 9 rotor diameters (0.58 km^2) to minimize turbine-turbine interference (*44*). The area for each wind reanalysis grid was divided by 0.58 km^2 to calculate the number of turbines in each grid. Grids with CFs less than 0.15 were considered uneconomical and were excluded accordingly. PE generation from wind in India was calculated using

$$A = \sum_{j=1}^{j=ng}\sum_{i=1}^{i=nh} P_{\mathrm{rated}} \times \mathrm{CF} \times \frac{A_j}{0.58} \quad (4)$$

where *ng* denotes the number of grids in India judged as feasible for deployment of wind power systems, *nh* represents number of operational hours for each year, and A_j refers to the area for each grid (in square kilometers).

We note that the wind power potential derived here is based on a fixed separation distance for wind turbines, whereas actual wind turbine

siting for specific wind farms would be optimized on the basis of the microlevel information on geographical topography and would yield a relatively higher source of electricity from the wind. Hence, we would argue that our results for the total wind power potential for India are relatively conservative. The interannual variation of available wind power, however, should be similar once the specific locations of the wind turbines are fixed. The main conclusions drawn here associated with the interannual variation and the long-term declining trend are not significantly influenced by this simplification.

Coupled numerical model experiments

To explore the physical mechanism responsible for declining wind speeds in India, we conducted a number of simulations using the WRF model version 3.8.1. The WRF model was developed by the National Centre for Atmospheric Research and has been shown to be capable of simulating monsoon circulation and other weather phenomena. The model domain was configured using Mercator projections extending from ~22°E to ~137°E (160 grid points) in the east-west direction and from 50°S to 50°N (160 grids) in the north-south direction, with a horizontal resolution of 81 km (fig. S4). According to the surface temperature trend in MERRA-2, SST increased by about 0.7° and 1.3°, respectively, in regions 1 (the EIO) and 2 (the SIO) over the study interval explored here. To examine the impacts of strong warming on wind potential in India in these two regions, we carried out three experiments: (i) a control simulation (WRF_{ctl}) with normal settings covering MJJA for 2001; (ii) SST increased by 0.7° over the EIO (WRF_{w1}); and (iii) SST increased by 0.7° and 1.3°over the EIO and SIO (WRF_{w1w2}), respectively. The differences between WRF_{w1} and WRF_{ctl} are interpreted as representing the response of the model to warming over the EIO, and the differences between WRF_{w1w2} and WRF_{ctl} are taken as indications of the response of the model to warming over both regions.

SUPPLEMENTARY MATERIALS

Supplementary material for this article is available at http://advances.sciencemag.org/cgi/content/full/4/12/eaat5256/DC1

Section S1. Datasets used to validate the trends in wind speeds derived from MERRA-2

Fig. S1. Zonal mean vertical pressure velocity during summer averaged over the 1980–2016 period inferred from MERRA-2.

Fig. S2. Long-term trend of wind speeds at 850 hPa (in m/s per year) inferred from MERRA-2 over the 1980–2016 interval.

Fig. S3. Trends of wind speeds in India inferred from multiple datasets.

Fig. S4. WRF modeling domain.

REFERENCES AND NOTES

1. International Energy Agency Statistics; www.iea.org/countries/non-membercountries/india/.
2. International Energy Agency, *India Energy Outlook: World Energy Outlook Special Report* (International Energy Agency, 2015); www.iea.org/publications/freepublications/publication/IndiaEnergyOutlook_WEO2015.pdf.
3. Global Wind Energy Council, *Indian Wind Energy: A Brief Outlook* (Global Wind Energy Council, 2016); www.gwec.net/wp-content/uploads/vip/GWEC_IWEO_2016_LR.pdf.
4. India Wind Turbine Manufacturers Association: Cumulative Wind Power Installation up to March 2017 (MW); www.indianwindpower.com/news_views.php#tab1.
5. Government of India Ministry of New and Renewable Energy; https://mnre.gov.in/renewable-energy-regulatory-framework.
6. X. Lu, M. B. McElroy, J. Kiviluoma, Global potential for wind-generated electricity. *Proc. Natl. Acad. Sci. U.S.A.* **106**, 10933–10938 (2009).
7. S. C. Pryor, R. J. Barthelmie, Climate change impacts on wind energy: A review. *Renew. Sustain. Energy Rev.* **14**, 430–437 (2010).
8. R. Schaeffer, A. S. Szklo, A. F. P. de Lucena, B. S. M. C. Borba, L. P. P. Nogueira, F. P. Fleming, A. Troccoli, M. Harrison, M. S. Boulahya, Energy sector vulnerability to climate change: A review. *Energy* **38**, 1–12 (2012).
9. K. B. Karnauskas, J. K. Lundquist, L. Zhang, Southward shift of the global wind energy resource under high carbon dioxide emissions. *Nat. Geosci.* **11**, 38–43 (2018).
10. P. Sherman, X. Chen, M. B. McElroy, Wind-generated electricity in China: Decreasing potential, inter-annual variability and association with changing climate. *Sci. Rep.* **7**, 16294 (2017).
11. G. He, A.-P. Avrin, J. H. Nelson, J. Johnston, A. Mileva, J. Tian, D. M. Kammen, SWITCH-China: A systems approach to decarbonizing China's power system. *Environ. Sci. Technol.* **50**, 5467–5473 (2016).
12. C. Moné, M. Hand, M. Bolinger, J. Rand, D. Heimiller, J. Ho, "2015 Cost of Wind Energy Review" (Technical Report NREL/TP-6A20-66861, National Renewable Energy Laboratory, 2017).
13. S. Gadgil, The Indian monsoon and its variability. *Annu. Rev. Earth Planet. Sci.* **31**, 429–467 (2003).
14. T. T. Fujita, K. Watanabe, T. Izawa, Formation and structure of equatorial anticyclones caused by large-scale cross-equatorial flows determined by ATS-I photographs. *J. Appl. Meteorol.* **8**, 649–667 (1969).
15. M. K. Roxy, K. Ritika, P. Terray, R. Murtugudde, K. Ashok, B. N. Goswami, Drying of Indian subcontinent by rapid Indian ocean warming and a weakening land-sea thermal gradient. *Nat. Commun.* **6**, 7423 (2015).
16. M. Roxy, Y. Tanimoto, B. Preethi, P. Terray, R. Krishnan, Intraseasonal SST-precipitation relationship and its spatial variability over the tropical summer monsoon region. *Clim. Dyn.* **41**, 45–61 (2013).
17. P. Swapna, R. Krishnan, J. M. Wallace, Indian Ocean and monsoon coupled interactions in a warming environment. *Clim. Dyn.* **42**, 2439–2454 (2014).
18. L. Dong, T. Zhou, The Indian Ocean sea surface temperature warming simulated by CMIP5 models during the twentieth century: Competing forcing roles of GHGs and anthropogenic aerosols. *J. Climate* **27**, 3348–3362 (2014).
19. L. Dong, T. Zhou, B. Wu, Indian Ocean warming during 1958–2004 simulated by a climate system model and its mechanism. *Clim. Dyn.* **42**, 203–217 (2014).
20. S. A. Rao, A. R. Dhakate, S. K. Saha, S. Mahapatra, H. S. Chaudhari, S. Pokhrel, S. K. Sahu, Why is Indian Ocean warming consistently? *Clim. Change* **110**, 709–719 (2012).
21. S.-K. Lee, W. Park, M. O. Baringer, A. L. Gordon, B. Huber, Y. Liu, Pacific origin of the abrupt increase in Indian Ocean heat content during the warming hiatus. *Nat. Geosci.* **8**, 445–449 (2015).
22. B. N. Goswami, V. Venugopal, D. Sengupta, M. S. Madhusoodanan, P. K. Xavier, Increasing trend of extreme rain events over India in a warming environment. *Science* **314**, 1442–1445 (2006).
23. Q. Jin, C. Wang, A revival of Indian summer monsoon rainfall since 2002. *Nat. Clim. Chang.* **7**, 587–594 (2017).
24. J. Ma, J.-Y. Yu, Paradox in South Asian summer monsoon circulation change: Lower tropospheric strengthening and upper tropospheric weakening. *Geophys. Res. Lett.* **41**, 2934–2940 (2014).
25. M. A. Bollasina, Y. Ming, V. Ramaswamy, Anthropogenic aerosols and the weakening of the South Asian summer monsoon. *Science* **334**, 502–505 (2011).
26. G. A. Meehl, J. M. Arblaster, W. D. Collins, Effects of black carbon aerosols on the Indian monsoon. *J. Climate* **21**, 2869–2882 (2008).
27. S. D. Sanap, G. Pandithurai, M. G. Manoj, On the response of Indian summer monsoon to aerosol forcing in CMIP5 model simulations. *Clim. Dyn.* **45**, 2949–2961 (2015).
28. R. Vautard, J. Cattiaux, P. Yiou, J.-N. Thépaut, P. Ciais, Northern Hemisphere atmospheric stilling partly attributed to an increase in surface roughness. *Nat. Geosci.* **3**, 756–761 (2010).
29. B. N. Goswami, M. S. Madhusoodanan, C. P. Neema, D. Sengupta, A physical mechanism for North Atlantic SST influence on the Indian summer monsoon. *Geophys. Res. Lett.* **33**, L02706 (2006).
30. S. Li, J. Perlwitz, X. Quan, M. P. Hoerling, Modelling the influence of North Atlantic multidecadal warmth on the Indian summer rainfall. *Geophys. Res. Lett.* **35**, L05804 (2008).
31. R. Lu, B. Dong, H. Ding, Impact of the Atlantic Multidecadal Oscillation on the Asian summer monsoon. *Geophys. Res. Lett.* **33**, L24701 (2006).
32. R. Zhang, T. L. Delworth, Impact of Atlantic multidecadal oscillations on India/Sahel rainfall and Atlantic hurricanes. *Geophys. Res. Lett.* **33**, L17712 (2006).
33. H. Holttinen, J. Kiviluoma, A. Forcione, M. Milligan, C. J. Smith, J. Dillon, J. Dobschinski, J. S. van Roon, N. Cutululis, A. Orths, P. B. Eriksen, "Design and operation of power systems with large amounts of wind power. Final summary report, IEA WIND Task 25, Phaser three 2012–2014" (VTT Technology, 2016).
34. MIT Energy Initiative, *Managing Large-Scale Penetration of Intermittent Renewables* (MIT Energy Initiative, 2011); https://energy.mit.edu/wp-content/uploads/2012/03/MITEI-RP-2011-001.pdf.
35. X. Chen, H. Zhang, Z. Xu, C. P. Nielsen, M. B. McElroy, J. Lv, Impacts of fleet types and charging modes for electric vehicles on emissions under different penetrations of wind power. *Nat. Energy* **3**, 413–421 (2018).

36. M. Zeyringer, J. Price, B. Fais, P.-H. Li, E. Sharp, Designing low-carbon power systems for Great Britain in 2050 that are robust to the spatiotemporal and inter-annual variability of weather. *Nat. Energy* **3**, 395–403 (2018).
37. S. Collins, P. Deane, B. Ó. Gallachóir, S. Pfenninger, I. Staffell, Impacts of inter-annual wind and solar variations on the European power system. *Joule* **2**, 2076–2090 (2018).
38. Experimental NOAA/ESRL PSD and CU CIRES Forecast in Global Tropics Domain; www.esrl.noaa.gov/psd/forecasts/sstlim/for4gl.html
39. E. Holt, J. Wang, Trends in wind speed at wind turbine height of 80 m over the contiguous United States using the North American Regional Reanalysis (NARR). *J. Appl. Meteorol. Climatol.* **51**, 2188–2202 (2012).
40. R. Gelaro, W. McCarty, M. J. Suárez, R. Todling, A. Molod, L. Takacs, C. A. Randles, A. Darmenov, M. G. Bosilovich, R. Reichle, K. Wargan, L. Coy, R. Cullather, C. Draper, S. Akella, V. Buchard, A. Conaty, A. M. da Silva, W. Gu, G.-K. Kim, R. Koster, R. Lucchesi, D. Merkova, J. E. Nielsen, G. Partyka, S. Pawson, W. Putman, M. Rienecker, S. D. Schubert, M. Sienkiewicz, B. Zhao, The Modern-Era Retrospective Analysis for Research and Applications, version 2 (MERRA-2). *J. Climate* **30**, 5419–5454 (2017).
41. X. Lu, M. B. McElroy, C. P. Nielsen, X. Chen, J. Huang, Optimal integration of offshore wind power for a steadier, environmentally friendlier, supply of electricity in China. *Energy Policy* **62**, 131–138 (2013).
42. NASA Land Processes Distributed Active Archive Center (LP DAAC), *MCD12C1: Land Cover Type Yearly L3 Global 500 m SIN Grid* (LP DAAC, 2012); https://lpdaac.usgs.gov/dataset_discovery/modis/modis_products_table/mcd12c1.
43. A. Jarvis, H. I. Reuter, A. Nelson, E. Guevara, "Hole-filled seamless SRTM dataV4" (International Centre for Tropical Agriculture, 2008); http://srtm.csi.cgiar.org.
44. M. R. Davidson, D. Zhang, W. Xiong, X. Zhang, V. J. Karplus, Modelling the potential for wind energy integration on China's coal-heavy electricity grid. *Nat. Energy* **1**, 16086 (2016).

Acknowledgments: We acknowledge the NASA Global Modeling and Assimilation Office for providing the MERRA-2 reanalysis dataset. **Funding:** This study was supported by the Harvard Global Institute. This research was supported also by State Key Laboratory on Smart Grid Protection and Operation Control of NARI Group, through the open topic project (20171613).
Author contributions: M.G., X.C., and M.B.M. conceived the research; M.G. and X.C. calculated the wind energy potential; Y.D., S.S., and X.L. assisted with the discussion; and all authors contributed to the final interpretation and writing of the manuscript, with major contributions from M.G., X.C., and M.B.M. **Competing interests:** The authors declare that they have no competing interests. **Data and materials availability:** All data needed to evaluate the conclusions in the paper are present in the paper and/or the Supplementary Materials. Additional data related to this paper may be requested from the authors.

Submitted 7 March 2018
Accepted 31 October 2018
Published 5 December 2018
10.1126/sciadv.aat5256

Citation: M. Gao, Y. Ding, S. Song, X. Lu, X. Chen, M. B. McElroy, Secular decrease of wind power potential in India associated with warming in the Indian Ocean. *Sci. Adv.* **4**, eaat5256 (2018).